Non-enzymatic roles of human RAD51 at stalled replication forks

Jennifer M. Mason[1,3,4*], Yuen-Ling Chan[1], Ralph W. Weichselbaum[1], and Douglas K. Bishop[1,3*]

[1]Department of Radiation and Cellular Oncology, [2]Department of Molecular Genetics and Cell Biology University of Chicago, Chicago, IL,

[3]Department of Genetics and Biochemistry, [4]Center for Human Genetics, Clemson University, Clemson, SC

Key words: DNA repair, replication, homologous recombination, RAD51

*Correspondence should be directed to:
Jennifer M Mason
Dept. of Genetics and Biochemistry
Clemson University
Robert F. Poole Agricultural Center, Room 154
130 McGinty Court
Clemson, SC 29634
Phone: (864) 656-3345
Email: jmason4@clemson.edu

Douglas K Bishop
Dept. of Radiation and Cellular Oncology
University of Chicago
Cummings Life Science Center, Box 13
920 E. 58th St.
Chicago, IL 60637
Phone: (773) 702-9211
Email: dbishop@uchicago.edu

Author contributions:
YLC purified RAD51 proteins and performed DNA binding assays and D-loop assay.
JMM performed all cell-based assays
JMM, YLC, RWW and DKB contributed to experimental design and preparation of the manuscript

ABSTRACT

The central recombination enzyme RAD51 has been implicated in replication fork processing and restart in response to replication stress. Here, we use a separation-of-function allele of RAD51 that retains DNA binding activity, but not strand exchange activity, to determine how RAD51 promotes replication fork stability. We find that cells lacking RAD51 strand exchange activity protect replication forks from MRE11-dependent degradation, and promote their conversion to a form that can be degraded by DNA2. We also provide evidence for both RAD51 strand exchange-dependent and strand exchange-independent mechanisms of replication restart.

INTRODUCTION

The complete and accurate replication of the genome is essential to maintain genome integrity. Replication forks face many obstacles that result in replication fork stalling or replication fork collapse. Proteins initially identified on the basis of their roles in homologous recombination (HR) are now known to have key functions during replication stress [1,2]. HR proteins act to protect and remodel stalled replication forks, and also to re-construct functional replication forks following fork collapse. As a result of these activities, HR proteins are critical to the ability of cells to restart stalled and collapsed replication forks.

The central HR protein, RAD51, forms helical nucleoprotein filaments on tracts of single strand DNA (ssDNA), such as those formed by nucleolytic processing of the DNA ends formed by DNA double strand breaks (DSBs). Once RAD51 filaments form on tracts of ssDNA, the protein alters the structure of the ssDNA, allowing the nucleoprotein filament to catalyze a homology search to identify an identical or nearly-identical sequence in duplex DNA, and then carry out exchange of the bound ssDNA strand with the "like" strand of the homologous duplex [3]. In this way, the homology search and strand exchange activity of RAD51 acts to form a homologous joint between a broken chromatid and its intact sister chromatid, leading to accurate repair of the DSB.

In addition to its role in repair of DSBs, RAD51 plays a role in DNA replication by promoting replication fork stability, as well as replication restart, under conditions of replication stress. Replication stress can be induced experimentally with drugs that block replication such as hydroxyurea (HU), which inhibits the production of nucleotide DNA precursors. Under conditions of replication stress, RAD51 promotes replication fork reversal[4,5]. Replication fork reversal involves branch migration in the direction opposite to replication forming a Holliday junction-containing "chicken foot" structure. Depletion of DNA2 increases the fraction of reversed forks with the regressed arm containing more dsDNA relative to ssDNA than observed in control cells[6]. This led to the model that DNA2 resection of a the reversed fork creates a ssDNA overhang that is a substrate for RAD51-mediated recombination[6]. Furthermore, DNA2 was responsible for the severe degradation phenotype observed in RECQ1-depleted cells, a helicase that is important in unwinding of regressed forks[6] as well as degradation of replication forks in wildtype cells. These results led to the conclusion that the exonuclease activity of DNA2 nuclease degrades reversed forks resulting in shortening of DNA tracts after treatment with HU [4,6]. RAD51 expression is required to generate the intermediate that promotes DNA2 degradation[6]. In addition to promoting fork reversal, RAD51 protects tracts of newly-synthesized "nascent" DNA from degradation; nascent ssDNA degradation occurs in cells with partial inhibition of RAD51 expression or activity in response a variety of DNA damage agents[7-10]. Nascent DNA degradation also occurs in cells lacking proteins required to load RAD51 on ssDNA such as BRCA1,BRCA2, FANCD2, and the RAD51 mediators including RAD51C and XRCC2 [5,7,11-14]. The degradation phenotype observed in these cells results from the inefficient loading and/or stabilization of RAD51 at the reversed fork[5,13-15]. A subset of the nucleases involved in DNA end resection, MRE11 and EXO1, are responsible for degradation of stalled forks in cells defective in RAD51 expression or RAD51 loading. Reversed forks are also substrates for cleavage by branch-specific nucleases such as MUS81, SLX4, and EEPD1, and cleavage of such forks is thought to be a mechanism leading to replication fork collapse following fork stalling [15-18]. These results indicate reversed forks undergo DNA2 degradation in response to replication stress, but are prone to pathological degradation by MRE11 and EXO1 in the absence of a stable RAD51

nucleoprotein filament. RAD51 is also required for the ability of the replication machinery to restart stalled or collapsed replication forks[19]. Although it is clear that RAD51 is required for protection of nascent DNA strands from MRE11, replication fork remodeling, and fork restart, the molecular mechanisms underlying each of these functions remains to be determined. One specific mechanistic question is: which of RAD51's functions during replication stress depend on its homology search and strand exchange activity, and which only require its ability to bind DNA? Here, we address this question using a mutant form of RAD51 that retains the ability to bind ssDNA, but lacks the ability to carry out strand exchange.

Our results provide evidence that the strand exchange activity of RAD51 is not required to protect stalled forks from MRE11 degradation. Surprisingly, we also show that strand exchange activity is not required for RAD51-dependent remodeling of stalled forks. In contrast, we find the strand exchange activity of RAD51 is required for efficient replication fork restart after HU treatment. Cytological analysis provides evidence that cells expressing a strand exchange-defective form of RAD51 accumulate DSBs and undergo frequent new origin firing in response to HU-induced replication stress. These observations lead us to model for the molecular pathways through which RAD51 contributes to the response to replication stress.

RESULTS

hsRAD51-II3A retains significant DNA binding activity, but is defective for D-loop formation.

To characterize the molecular functions of human RAD51's DNA binding and strand exchange activities during replication stress, we constructed an allele of human RAD51 corresponding to the *S. cerevisiae rad51-II3A* allele [20]. The budding yeast Rad51-II3A protein retains DNA binding, but not strand exchange activity (see Methods for details concerning the human RAD51-II3A construct). The corresponding human RAD51-II3A (hsRAD51-II3A) protein has 3 amino acid residues, R130, K303, and R310 changed to alanines. To determine if the mutant human protein (hsRAD51-II3A) had the same properties as its budding yeast counterpart, we purified hsRAD51-WT and hsRAD51-II3A proteins after

expression in *E. coli* (Supplemental Figure 1a). We then analyzed the nucleoprotein filament forming and strand exchange activities of the two forms of RAD51 using biochemical assays. Using fluorescence polarization (FP), we measured binding of the two forms of the protein to a Alexa84-tagged 88-nt ssDNA oligo [9]. Titration showed that the two proteins have similar binding activities to this oligo, the apparent Kd's for hsRAD51-WT and hsRAD51-II3A were 57 ± 1 nM and 132 ± 5 nM, respectively (Figure 1a). Thus, hsRAD51-II3A displays only a modest DNA binding defect in this assay. Next, we examined the homology search and strand exchange activity of hsRAD51-II3A with a D-loop assay that employs a 90-nt single strand oligonucleotide and a 4.4-kb supercoiled plasmid carrying a dsDNA sequence identical to the sequence of the oligonucleotide (Figure 1b). In this assay, hsRAD51-II3A exhibited 840-fold less D-loop activity compared to hsRAD51-WT (0.06% vs. 17% of plasmid DNA forming D-loops, respectively). Together the results demonstrate that, like its budding yeast counterpart, hsRAD51-II3A retains DNA binding, but not strand exchange activity, *in vitro*.

Next, we asked if hsRAD51-II3A displays separation of RAD51's DNA binding and HR functions *in vivo*. hsRAD51-WT and hsRAD51-II3A were expressed in U2OS cells and the expression of the endogenous RAD51 protein was repressed via siRNA targeting of the 3'UTR of the RAD51 mRNA. In addition to transfection of the construct expressing siRNA resistant hsRAD51-WT, a second positive control was carried out by transfection of non-silencing siRNA (siNS). Treatment with RAD51 siRNA reduced expression of the endogenous protein to less than 7% of that observed in the siNS control (Supplemental Figure 1b). Following transfection of RAD51 cDNA plasmid constructs that lacked 3'UTR sequences subject to siRNA targeting, both hsRAD51-WT and hsRAD51-II3A were expressed at the same level, which was ~5 fold higher than that seen for the endogenous protein in the non-silencing siRNA (siNS) control (see Supplemental Figure 1b).

To determine the extent to which the spontaneous distribution of RAD51 differed in cells transfected with RAD51 expression constructs from that observed with endogenous RAD51, we immunostained cells from growing cultures for RAD51 and counted RAD51 foci in unselected nuclei. RAD51 typically forms a small number of nuclear immunostaining foci in the absence of induced

damage. These foci either mark sites of spontaneous DNA damage or the sites of non-repair-associated RAD51 oligomers. Cells expressing hsRAD51-WT contained on average 1.5±6.7 RAD51 foci/cell and hsRAD51-II3A contained 1.5±4 RAD51 foci/cell, compared to 0.7±1.8 foci/cell in siNS cells; Figure 1d). In addition, a small subpopulation of hsRAD51-WT and hsRAD51-II3A (3.4±1.5% and 2.3±1.3%, respectively) transfected cells contained an average of 44±14 elongated RAD51 fibers with contour lengths of 0.5 to 3 microns long (Supplemental Figure 1c). This type of staining pattern was observed previously as a consequence of high levels of RAD51 overexpression and reflects binding of RAD51 to undamaged DNA[10]. This analysis indicated that the level of expression of RAD51 from transfection of siRNA resistant constructs causes only a slight increase in the frequency of spontaneous foci in 96-98% of transfected cells.

Analysis of damage induced RAD51 foci provided evidence that hsRAD51-II3A retains DNA binding activity *in vivo*. RAD51 forms nucleoprotein filaments on the 3' ssDNA overhang resulting from formation and strand-specific resection of DNA double strand breaks. Loading of RAD51 on ssDNA tracts *in vivo* is conventionally assayed by immunostaining for RAD51 and measuring the number and of RAD51 foci resulting from treatment of cells with agents that induce DNA breaks, such as x-rays [21-24]. As expected, the number of RAD51 foci significantly increased after x-ray treatment of siNS transfected cells (Figure 1c,d; 11±14.4 foci/cell IR *vs* 0.7±1.8 foci/cell). Cells depleted of RAD51 exhibited a 4-fold reduction in IR-induced RAD51 focus formation (2.5±6 foci/cell; $p<0.005$). Cells transfected with hsRAD51-WT (9±9.7 foci/cell) following siRNA for endogenous RAD51 showed the same level of x-ray induced foci as the siNS control (11±14.4 foci/cell), further validating the system. Importantly, the number of IR-induced hsRAD51-II3A (9±8.3) foci also did not differ significantly from siNS (11±14.4) or hsRAD51-WT (9±9.7) controls. Together, these results indicate hsRAD51-II3A retains significant DNA binding activity *in vivo*.

To determine if hsRAD51-II3A is defective in HR, we employed the DR-GFP assay[12]. In this assay, HR generates a functional GFP allele following induction of a chromosomal DNA break in one of the two defective copies of GFP carried by the reporter cell line (Supplemental Figure 1d). Double

strand breaks were induced in the U2OS-DR-GFP cells by transfection with a plasmid expressing the I-SceI endonuclease. HR efficiency was then measured by flow cytometry as the frequency of GFP expressing cells. RAD51 depletion reduced HR efficiency 6-fold compared to siNS controls (0.97±0.1% GFP positive cells siNS vs 0.16±0.03% siRAD51; p-value<0.05; Figure 1e). Expression of hsRAD51-WT in RAD51 depleted cells increased the HR efficiency by 3-fold compared to siRAD51 cells (0.49±0.03 GFP positive cells vs. 0.16±0.03% siRAD51; p-value<0.005). In contrast, hsRAD51-II3A did not increase HR efficiency in RAD51-depleted cells (0.12±0.09 % GFP positive cells vs. 0.16±0.03%; p-value=0.6) indicating hsRAD51-II3A is defective for HR-mediated repair of DSBs. Together, these data indicate human hsRAD51-II3A is able to form RAD51 nucleoprotein filaments with normal efficiency, but is defective for HR *in vivo,* consistent with our biochemical observations.

hsRAD51-II3A protects nascent DNA strands from MRE11 degradation and promotes DNA2 degradation of stalled replication forks

We next sought to elucidate the molecular function of RAD51's strand exchange activity during perturbed replication, using the DNA fiber assay to measure the ability of cells treated with the replication inhibitor HU to protect nascent DNA strands from degradation. Upon replication fork reversal, degradation of nascent strands occurs through two mechanistically distinct pathways. Pathways with defects in RAD51 loading and/or stabilization of RAD51 nucleoprotein filaments are degraded by the nuclease MRE11 [5,7,11,13,14]. Prolonged exposure to HU (4 mM HU for 8 hours) was previously shown to result in nascent strand degradation in HR-proficient cells by the nuclease DNA2[6]. Unlike the pathological degradation of nascent strands by MRE11, which is inhibited by RAD51, degradation by DNA2 is promoted by RAD51 and is thought be important for replication fork restart[6]. The ability of RAD51 to promote replication fork reversal has been proposed to require the protein's strand exchange activity [4,19]. To test this proposal, we examined hsRAD51-II3A expressing cells to determine if strand exchange activity of RAD51 is required to promote DNA2-mediated degradation or prevent MRE11-dependent degradation following 8 hours of HU treatment. siNS and siRAD51 treated cells transfected

with siRNA resistant hsRAD51-WT served as positive controls, and siRAD51 treated cells transfected with empty vector served as negative control. Consistent with previous reports, we observed shortening of nascent DNA strands in siNS and hsRAD51-WT controls at 8 hours (14.7±5.8 μm vs 11.7±4.9 μm; *p*-value<0.005 for siNS, and 17.2±5.7 μm vs. 14.2±4.8 μm; *p*-value<0.005 for hsRAD51-WT, Figure 2a). Reducing expression of DNA2 via siRNA treatment restored the average tract length to that observed without HU treatment (Figure 2a; Supplemental Figure 2a). Treatment of the same cells with mirin did not result in a significant change in average tract length. These results confirm that DNA2 is responsible for the shortening of nascent strands under these conditions. The average tract length of nascent DNA in controls cells depleted of RAD51 did not result in shortening of DNA tract lengths under any conditions treated with HU (Figure 2a). These findings confirm that RAD51 remodels HU stalled replication forks to provide a substrate for DNA2-mediated degradation and MRE11-dependent degradation[6,13]. Treatment of RAD51C-deficient fibroblasts with HU resulted in significant shortening of replication tracts that was restored upon mirin treatment confirming that proteins required to load or stabilize RAD51 is required to protect forks from MRE11degradation[12] (Supplemental Figure 2b). The results with hsRAD51-II3A expressing cells were nearly identical to the positive controls; nascent tract lengths were reduced following prolonged HU treatment from 18±6.3 μm to 12.8±5.1 μm, and siDNA2, but not mirin, prevented this reduction.

To confirm this result, we examined fork degradation by pulsing cells with CldU followed by IdU before treatment with HU for 8 hours and measured the ratio of IdU to CldU (Figure 2b). Consistent with a reduction in tract length, siNS and hsRAD51-WT expressing cells exhibited a significant reduction in the CldU:IdU ratio (0.68±0.26 μm to 0.48±0.20 μm for siNS *p*-value <0.005, 0.71±0.22 μm to 0.46±0.20 μm for hsRAD51-WT *p*-value <0.005). Reducing DNA2 expression restored ratios to those observed in untreated samples. In contrast, treatment with mirin did not result in a significant change in the CldU:IdU ratio in either siNS or hsRAD51-WT expressing cells. Consistent with RAD51 fork reversal and therefore preventing MRE11 or DNA2 degradation, depletion of RAD51

did not result in tract degradation under any treatment condition. Consistent with the result above, hsRAD51-II3A expressing cells exhibited a significantly reduced CldU:IdU ratio (0.75±0.62 μm to 0.62±0.30 μm, *p*-value <0.005) that is restored in cells depleted for DNA2. Treatment with mirin has no effect on the CldU:IdU ratio in hsRAD51-II3A expressing cells. In contrast to expectation, these data indicate that the strand exchange activity of RAD51 is not required to remodel stalled replication forks to a form that is sensitive to DNA2-mediated degradation.

RAD51 strand exchange activity is required for replication fork restart after prolonged HU treatment

Previous studies showed RAD51 is required for restart of replication forks stalled by HU treatment[7]. Thus, we determined if the strand exchange activity of RAD51 is required to restart stalled replication forks after treatment with HU for 5 and 8 hours (Figure 3). Cells were pulsed with CldU, treated with HU for 5 and 8 hours, and then the HU in the medium was replaced with a second fluorescence DNA precursor, IdU, to detect DNA synthesized after HU treatment. Replication forks that successfully restart after removal of HU are visible as adjacent CldU and IdU replication tracts. The siNS and hsRAD51-WT transfected cells showed significant levels of restart after both 5 and 8 hours of HU treatment; in siNS control cells 50±8 % and 39±3.9 % of replication forks restarted after 5 and 8 hours of HU treatment respectively; in hsRAD51-WT transfected cells, the corresponding numbers were 48±3.3% and 40±3.9% respectively. Depletion of RAD51 resulted in a 2-fold reduction in the frequency of restart at 5 hours (24.3±4.8% fork restart; $p<0.005$) and a 2.3-fold reduction at 8 hours (17.1±2.4% fork restart; $p<0.005$), confirming that RAD51 is required for efficient fork restart after HU treatment. hsRAD51-II3A expressing cells gave results that were intermediate between the positive and negative controls, with only a slight decrease in the efficiency of replication fork restart (44±2.6%; $p<0.05$) at 5 hours and a more severe (2.8-fold) reduction in the frequency of restart after 8 hours HU treatment (13.8±2.7% fork restart; $p<0.005$). Thus, RAD51's strand exchange activity is required for

efficient replication restart, with a much greater requirement after 8 hours as compared to 5 hours of HU treatment. The results also raise the possibility that the strand exchange defective form of RAD51 can promote more restart than occurs when RAD51 levels are dramatically repressed. The alternative possibility is that hsRAD51-II3A has residual strand exchange activity *in vivo*, in spite of our inability to detect such activity biochemically. However, this seems unlikely because hsRAD51-II3A did not exhibit higher HR activity *in vivo* using the DR-GFP assay compared to RAD51-depleted cells (Figure 1).

Next, we examined cells for new origin firing following a period of replication blockage by HU. New origin firing can be detected in the same double labeling experiments described above, by the presence of tracts containing only IdU labeling. We observed very little or no new origin firing (<5%) in the positive and negative control experiments (Figure 3). After 5 hours HU treatment, hsRAD51-II3A cells exhibited new origin firing similar to control cell lines. In contrast, hsRAD51-II3A expressing cells exhibited a 19-fold higher level of new origin firing at 8 hours (19±2.7%; $p<0.005$). These data indicate that replication fork blockage by HU leads to more new origin firing in cells expressing hsRAD51-II3A, than occurs in cells expressing hsRAD51-WT or in cells blocked for RAD51 expression.

53BP1 foci accumulate in hsRAD51-II3A cells after HU treatment

Replication fork blockage by HU can lead to fork collapse, a process that creates a broken DNA end that recruits DNA break proteins including 53BP1[25-29]. Although one study speculated 53BP1 may form small foci by binding to DNA ends of reversed forks [28], three other studies did not report activation of the double strand break response under conditions of fork reversal[4,17,29]. Replication stress-induced fork collapse and associated DNA break signaling have been shown to lead to the firing of new origins[19]. Given prior evidence for a functional association between new origin firing and fork collapse, we hypothesized that the new origin firing we observed in HU-treated hsRAD51-II3A cells is a consequence of higher levels of collapsed fork accumulation. We therefore tested for evidence of

collapsed fork accumulation specifically in S phase cells by staining with the DSB-specific marker 53BP1 and the replication fork specific marker PCNA [30,31]. After 8 hours in HU, the siNS and hsRAD51-WT positive controls, and the siRAD51 negative control, showed a modest 1.6-fold increase in the average number of 53BP1 foci /cell (10.3±6.5 53BP1 foci/cell compared to 6.4±3.8 foci per cell prior to HU treatment; Figure 4). Importantly, expression of hsRAD51-II3A cells resulted in a significantly greater (2.5-fold) increase in 53BP1 foci after 8 hours HU treatment (18.7±0.8 53BP1 foci/cell; p-value<0.005). As a control against the possibility that 53BP1 activity differs between cultures, a fraction of each culture was treated with HU for 24 hours. This highly prolonged replication arrest caused equivalent induction of 53BP1 foci in all samples, as expected (Supplemental Figure 3). Together, the results suggest that hsRAD51-II3A causes more accumulation of collapsed forks following 8 hr HU treatment than occurs in cells expressing equivalent levels of hsRAD51-WT, and also more than in cells expressing very low levels of RAD51. The possible mechanistic basis for these observations is discussed below.

DISCUSSION

RAD51 has been implicated in several steps in response to replication stress including fork protection, replication fork remodeling, and replication fork restart. Here, we utilized a RAD51 mutant allele that retains DNA binding activity, but is defective in strand exchange to gain mechanistic insight into the role of RAD51 at stalled replication forks. Previous studies have suggested that stabilization of RAD51 filaments is sufficient to protect from MRE11 dependent-degradation[7,11]. Consistent with this model, we found that the ability of RAD51 to protect nascent strands from MRE11-mediated degradation is independent of strand exchange activity. Our results provide additional insight into the mechanism of RAD51-dependent replication fork remodeling by showing that degradation of nascent DNA by DNA2 does not require RAD51's strand exchange activity. We further show that the strand exchange activity of RAD51 is required for efficient replication restart, although some restart appears to be independent of RAD51.

Like RAD51[6,32], the *E. coli* recombinase RecA has been implicated in promoting fork reversal in response to replication stress. Purified RecA can convert a model replication fork substrate to a reversed fork structure *in vitro*[33]. *In vivo* experiments provided evidence for both RecA-dependent and RecA-independent formation of reversed forks. In response to ultraviolet (UV) light, RecA maintains the integrity of reversed forks by protecting against degradation by RecJ or RecQ[34]. In cells with inactivated DnaB helicase, RecA was shown to catalyze replication intermediates that were cleaved by the Holliday junction resolvases RuvABC, indicating RecA is required for fork reversal[35]. However, in mutants defective in the helicase Rep, intermediates cleaved by RuvABC formed in a RecA-independent manner [35]. Thus, there are both RecA-dependent and RecA-independent pathways for fork reversal in *E. coli*. It remains to be determined if RecA's strand exchange activity is required for replication fork reversal in wild type cells.

DNA2-dependent degradation of replication forks occurs as a consequence of RAD51-dependent replication fork reversal[6]. Here, we provide evidence that the strand exchange activity of RAD51 is not required to promote DNA2-dependent degradation of stalled forks, suggesting reversal of replication forks is dependent on DNA binding activity of RAD51 and not strand exchange activity. How can the DNA binding activity of RAD51 promote replication fork reversal? RAD51 interacts with polymerase α preventing the formation of ssDNA gaps at stalled forks [14]. If annealing of complementary nascent strands is important to drive fork reversal, RAD51 preventing significant ssDNA formation at the fork may be sufficient to drive fork reversal. Replication forks can reverse spontaneously *in vitro* due to accumulation of positive supercoiling ahead of a replication fork [36]. The extent to which spontaneous fork reversal occurs in wild type cells is unclear, but accumulation of positively supercoiled DNA due to Topoisomerase I inhibition also causes fork reversal, suggesting supercoiling alone can drive fork reversal *in vivo* [29]. A second mechanism through which DNA-bound RAD51 could promote fork reversal is by recruiting other proteins that act directly to catalyze the process. RAD54 [37], FANCM[38], HTLF[39], and ZRANB3[40,41], have been found to be able to reverse a model replication fork substrate in vitro and FBH1, SMARCL1, HLTF, and ZRANB3 have been shown to promote fork reversal *in*

vivo[13,14,42,43]. Finally, it is possible that RAD51 strand exchange activity promotes fork reversal, but in the absence of RAD51 strand exchange activity (e.g. hsRAD51-II3A), additional proteins are able to bind and promote fork reversal. Further studies will be required to determine if binding of RAD51 at stalled forks influences the fork reversal activity of other proteins that could contribute more directly to reversal.

hsRAD51-II3A cells promoted significant restart after 5 hours HU treatment, but were highly defective in replication restart after longer (8 hours) treatment with HU. Together, our results lead us to a model for three distinct pathways to restart stalled replication forks, one that is RAD51-dependent, strand exchange-dependent; a second that is RAD51-dependent, strand exchange-independent; and a third that is RAD51-independent. Thus, replication fork protection and replication fork restart are mechanistically distinct events. Further, our results indicate that the RAD51-dependent, strand exchange-dependent mechanism is more predominant after 8 hours of exposure to HU as compared to 5 hours of exposure, while the converse is true for the RAD51-dependent, strand exchange-independent mechanism. Our results are consistent with work using an allele of *S pombe rad51* that was modelled on the *S. cerevisiae* allele, but not biochemicaly characterized. That work led to the proposal that strand exchange activity coded by *S. pombe rad51*$^{+}$ is dispensable for replication fork protection from Exo1, but required for efficient fork restart[44].

Combining all the data, we propose the following model for RAD51-dependent replication fork remodeling and restart (Figure 5). At early times after fork blockage, binding of RAD51 to DNA is sufficient to protect the replisome by preventing excessive uncoupling of the replication fork; thereby preventing significant ssDNA accumulation. RAD51 loading directly to reversed forks blocks access of the DNA to MRE11. When the replication block is removed, reversed forks can be resolved by the action of helicases such as RECQ1, reinstating the replication fork[45]. In contrast, prolonged stalling of a replication fork results in the formation of an intermediate that usually requires the strand exchange activity of RAD51 for restart. One possibility is that DNA2-mediated resection of the "middle toe" of the reversed fork provides a single-stranded overhang that serves as a substrate for formation of a

RAD51 nucleoprotein filament. In this instance, RAD51-mediated strand invasion is used to reinstate the replication fork. Alternatively, endonucleolytic cleavage of reversed fork intermediates by nucleases such as MUS81 and SLX4 may form collapsed fork structures containing single-ended DNA breaks [16,17]. These structures are expected to require RAD51-mediated strand exchange to restore functional forks [19]. Consistent with this, hsRAD51-II3A expressing cells accumulate markers for un-resolved DNA ends and exhibit increased origin firing. These phenotypes are associated with the accumulation of collapsed replication forks[19]. Interestingly, the collapsed fork-associated phenotypes observed in hsRAD51-II3A expressing cells are more severe than those observed in RAD51 depleted cells. This observation suggests that replication fork remodeling mediated by hsRAD51-II3A traps intermediates that cannot be resolved by RAD51 strand exchange-independent pathways before or after the conversion of reversed forks to collapsed forks. Recent studies have indicated RAD52 can restart forks in the absence of RAD51 and BRCA2 though a break-induced replication mechanism [46,47]. We speculate the RAD51-independent replication fork restart observed at 5 hours HU depends on RAD52 activity.

Here, we demonstrate RAD51 DNA binding activity alone is sufficient for replication fork protection and remodeling, but strand exchange activity is required for replication fork restart. Future work will determine precisely what types of replication intermediates require the strand exchange activity of RAD51. It will also be of interest to determine if strand exchange activity of RAD51 has additional roles at replication forks under conditions which require repair of a physical lesion (e.g. interstrand crosslinks), or conditions that only result in a moderate reduction in replication fork speed (e.g. UV-light induced damage) [10,48].

ACKNOWLEDGEMENTS

This work is funded by the National Institutes of Health grants GM50936 to YLC and DKB and CA205518-01 to JMM and DKB. We also would like to thank Alessandro Vindigni for providing feedback on the manuscript.

ONLINE MATERIAL AND METHODS

Expression and purification of hsRAD51-WT and hsRAD51-II3A mutant. The open reading frames of hsRAD51-WT and hsRAD51-II3A mutant with a C-terminal His-6 tag were cloned into pET21d (Novagen). The proteins were overexpressed in *E. coli* Rosetta(DE3) plysS cells by induction using 0.5 mM IPTG. The expression and purification were as detailed previously for protein yeast Dmc1 [49].

Binding assay: The binding of hsRAD51 to ssDNA was assayed by the fluorescence polarization method as described previously[50] with the following modifications. An 84-mer ssDNA conjugated with Alexa Flour-488 at the 5' end (sequence: 5'-GGTAGCGGTTGGGTGAGTGGTGGGGAGGGTCGGGAGGTGGCGTAGAAACATGATAGGAATGTGAATGAATGAAGTACAAGTAAA-3'; synthesized by Integrated DNA Technologies) was used at 200 nM nucleotides (2.4 nM). The binding reactions were performed at 37˚C for 30 minutes in buffer B (25 mM Tris-HCl (pH 7.8), 1 mM $MgCl_2$, 1 mM ATP, 1 mM DTT, 50 mM $NaCl_2$, 50 µM $CaCl_2$, and 100 µg/ml BSA). The fluorescence polarization (in mP units) was measured using a Tecan Infinite F200 PRO plate reader. All binding conditions were performed in triplicate, and the mean values were plotted with standard deviation. Buffer and ssDNA had no effect on fluorescence polarization in the absence of added protein (data not shown). The first data point on the graph contains 10 nM protein.

D-loop assay. The assay was performed essentially as described previously [8]. Reactions were carried out in 25 mM Tris-HCl (pH 7.8); 1 mM $MgCl_2$, 1 mM ATP, 1 mM DTT, 50 µM $CaCl_2$, and 100 µg/ml BSA; ssDNA (90 mer sequence 5'TACGAATGCACACGGTGTGGTGGGCCCAGGTATTGTTAGCGGTTTGAAGCAGGCGGCAGAAGAAGTAACAAAGGAACCTAGAGGCCTTTT) was used at 3.6 µM nucleotide or 40 nM); negative supercoiled plasmid was pRS306 at 5 nM (22 µM bp).

Cell culture. U2OS DR-GFP cells were grown in DMEM (Gibco) supplemented with 10% Fetal Bovine Serum.

Expression of RAD51 in U2OS cells. WT RAD51 or RAD51 cDNA containing mutations in the secondary binding site (R130A, K303A, R310A) was cloned into pcDNA 3.1 (Invitrogen) using Gibson assembly per manufacturer's instructions (New England Biolabs). U2OS cells were transfected with pcDNA3.1, hsRAD51-WT (pNRB707), or hsRAD51-II3A (pNRB708) expression plasmids using Lipofectamine 3000 (Invitrogen) as per manufacturer's instructions. After 24 hours, cells were transfected with RAD51 siRNAs targeting the 3'UTR. At 48 hours post transfection, cells were collected and analyzed for the various assays.

siRNA sequences. siRNAs were transfected using Lipofetamine RNAiMAX as per manufacturer's instructions (Invitrogen). The All-Star negative control (siNS) siRNA was used as a control (Qiagen). The following siRNA sequences were used in this study.

siRAD51 5' GACUGCCAGGAUAAAGCUU was used in a previous study [51].

siDNA2 5' CAGUAUCUCCUCUAGCUAG was used in a previous study [6].

Nascent DNA fiber assay. Cells were pulsed with CldU (50 μM), or CldU (50 μM) followed by IdU (150 μM) were treated with HU (4mM) for the indicated times. Tract lengths were measured using Image J. To measure replication restart, cells were pulsed with CldU (50 μM) before treatment with 4mM HU for the indicated times. HU was removed and cells were pulsed with IdU (50 μM). Mirin (50 μM) was added 30 minutes prior to the pulse with CldU and was present throughout the experiment. The nascent DNA fiber assay was performed as previously described[21]. At least 150 replication tracts were measured for each condition from at least two independent experiments. Statistical significance was determined using Mann-Whitney U test.

RAD51 and 53BP1 focus formation. 48 hours after transfection with siRNAs, cells were treated with 4 mM HU for the indicated times. For RAD51 focus formation, cells were treated with 6 Gy using a maxitron x-ray generator. Cells were fixed and stained as previously described[21]. Antibodies used in this study are as followed: RAD51 is a rabbit polyclonal antibody against purified human RAD51 (1:1000, Pacific Immunology). 53BP1 (1:1000, NB100-304) was from Novus Biologicals and PCNA (1:1000, IG7) was from Abnova. Statistical significance was determined by the Wilcoxon Rank Sum Test.

Western blotting. Western blotting was done as previously described[52]. Anti-DNA2 (1:500; ab96488) was from Abcam. Proteins were detected using a C-DIGIT blot scanner (Licor).

DR-GFP assay. U2OS cells containing the DR-GFP construct stably integrated into the genome were transfected with a plasmid expressing I-SceI (pBAS) or an empty vector (pCAGG) after the indicated treatments[53]. After 48 hours, cells were collected and the percentage of cells expressing GFP was determined by flow cytometry (LSR II, BD Biosciences). Statistical significance was determined using a t-test.

REFERENCES

1. Kolinjivadi, A. M. *et al.* Moonlighting at replication forks - a new life for homologous recombination proteins BRCA1, BRCA2 and RAD51. *FEBS Lett.* **47,** 222 (2017).

2. Berti, M. & Vindigni, A. Replication stress: getting back on track. *Nat. Struct. Mol. Biol.* **23,** 103–109 (2016).

3. San Filippo, J., Sung, P. & Klein, H. Mechanism of eukaryotic homologous recombination. *Annu. Rev. Biochem.* **77,** 229–257 (2008).

4. Zellweger, R. *et al.* Rad51-mediated replication fork reversal is a global response to genotoxic treatments in human cells. *J. Cell Biol.* **208,** 563–579 (2015).

5. Mijic, S. *et al.* Replication fork reversal triggers fork degradation in BRCA2-defective cells. *Nat Commun* **8,** 859 (2017).

6. Thangavel, S. *et al.* DNA2 drives processing and restart of reversed replication forks in human cells. *J. Cell Biol.* **208,** 545–562 (2015).

7. Schlacher, K. *et al.* Double-strand break repair-independent role for BRCA2 in blocking stalled replication fork degradation by MRE11. *Cell* **145,** 529–542 (2011).

8. Spies, J. *et al.* Nek1 Regulates Rad54 to Orchestrate Homologous Recombination and Replication Fork Stability. *Mol. Cell* **62,** 903–917 (2016).

9. Su, F. *et al.* Nonenzymatic role for WRN in preserving nascent DNA strands after replication stress. *Cell Rep* **9,** 1387–1401 (2014).

10. Vallerga, M. B., Mansilla, S. F., Federico, M. B., Bertolin, A. P. & Gottifredi, V. Rad51 recombinase prevents Mre11 nuclease-dependent degradation and excessive PrimPol-mediated elongation of nascent DNA after UV irradiation. *Proc. Natl. Acad. Sci. U.S.A.* **112,** E6624–33 (2015).

11. Schlacher, K., Wu, H. & Jasin, M. A distinct replication fork protection pathway connects Fanconi anemia tumor suppressors to RAD51-BRCA1/2. *Cancer Cell* **22,** 106–116 (2012).

12. Somyajit, K., Saxena, S., Babu, S., Mishra, A. & Nagaraju, G. Mammalian RAD51 paralogs protect nascent DNA at stalled forks and mediate replication restart. *Nucleic Acids Res.* **43,** 9835–9855 (2015).

13. Taglialatela, A. *et al.* Restoration of Replication Fork Stability in BRCA1- and BRCA2-Deficient Cells by Inactivation of SNF2-Family Fork Remodelers. *Mol. Cell* **68,** 414–430.e8 (2017).

14. Kolinjivadi, A. M. *et al.* Smarcal1-Mediated Fork Reversal Triggers Mre11-Dependent Degradation of Nascent DNA in the Absence of Brca2 and Stable Rad51 Nucleofilaments. *Mol. Cell* **67,** 867–881.e7 (2017).

15. Lemaçon, D. *et al.* MRE11 and EXO1 nucleases degrade reversed forks and elicit MUS81-dependent fork rescue in BRCA2-deficient cells. *Nat Commun* **8,** 860 (2017).

16. Couch, F. B. *et al.* ATR phosphorylates SMARCAL1 to prevent replication fork collapse. *Genes Dev.* **27,** 1610–1623 (2013).

17. Neelsen, K. J., Zanini, I. M. Y., Herrador, R. & Lopes, M. Oncogenes induce genotoxic stress by mitotic processing of unusual replication intermediates. *J. Cell Biol.* **200,** 699–708 (2013).

18. Wu, Y. *et al.* EEPD1 Rescues Stressed Replication Forks and Maintains Genome Stability by Promoting End Resection and Homologous Recombination Repair. *PLoS Genet.* **11,** e1005675 (2015).

19. Petermann, E., Orta, M. L., Issaeva, N., Schultz, N. & Helleday, T. Hydroxyurea-stalled replication forks become progressively inactivated and require two different RAD51-mediated pathways for restart and repair. *Mol. Cell* **37,** 492–502 (2010).

20. Cloud, V., Chan, Y.-L., Grubb, J., Budke, B. & Bishop, D. K. Rad51 is an accessory factor for Dmc1-mediated joint molecule formation during meiosis. *Science* **337,** 1222–1225 (2012).

21. Mason, J. M. *et al.* RAD54 family translocases counter genotoxic effects of RAD51 in human tumor cells. *Nucleic Acids Res.* **43,** 3180–3196 (2015).

22. Haaf, T., Golub, E. I., Reddy, G., Radding, C. M. & Ward, D. C. Nuclear foci of mammalian Rad51 recombination protein in somatic cells after DNA damage and its localization in synaptonemal complexes. *Proc. Natl. Acad. Sci. U.S.A.* **92,** 2298–2302 (1995).

23. Raderschall, E., Golub, E. I. & Haaf, T. Nuclear foci of mammalian recombination proteins are located at single-stranded DNA regions formed after DNA damage. *Proc. Natl. Acad. Sci. U.S.A.* **96,** 1921–1926 (1999).

24. Bishop, D. K. *et al.* Xrcc3 is required for assembly of Rad51 complexes in vivo. *J. Biol. Chem.* **273,** 21482–21488 (1998).

25. Groth, P. *et al.* Methylated DNA causes a physical block to replication forks independently of damage signalling, O(6)-methylguanine or DNA single-strand breaks and results in DNA damage. *J. Mol. Biol.* **402,** 70–82 (2010).

26. Fedor, Y. *et al.* From single-strand breaks to double-strand breaks during S-phase: a new mode of action of the Escherichia coli Cytolethal Distending Toxin. *Cell. Microbiol.* **15,** 1–15 (2013).

27. Jones, R. M., Kotsantis, P., Stewart, G. S., Groth, P. & Petermann, E. BRCA2 and RAD51 promote double-strand break formation and cell death in response to gemcitabine. *Mol. Cancer Ther.* **13,** 2412–2421 (2014).

28. Ray Chaudhuri, A., Ahuja, A. K., Herrador, R. & Lopes, M. Poly(ADP-ribosyl) glycohydrolase prevents the accumulation of unusual replication structures during unperturbed S phase. *Mol. Cell. Biol.* **35,** 856–865 (2015).

29. Ray Chaudhuri, A. *et al.* Topoisomerase I poisoning results in PARP-mediated replication fork reversal. *Nat. Struct. Mol. Biol.* **19,** 417–423 (2012).

30. Bravo, R. & Macdonald-Bravo, H. Existence of two populations of cyclin/proliferating cell nuclear antigen during the cell cycle: association with DNA replication sites. *J. Cell Biol.* **105,** 1549–1554 (1987).

31. Schultz, L. B., Chehab, N. H., Malikzay, A. & Halazonetis, T. D. p53 binding protein 1 (53BP1) is an early participant in the cellular response to DNA double-strand breaks. *J. Cell Biol.* **151,** 1381–1390 (2000).

32. Yoon, D., Wang, Y., Stapleford, K., Wiesmüller, L. & Chen, J. P53 inhibits strand exchange and replication fork regression promoted by human Rad51. *J. Mol. Biol.* **336,** 639–654 (2004).

33. Robu, M. E., Inman, R. B. & Cox, M. M. RecA protein promotes the regression of stalled replication forks in vitro. *Proc. Natl. Acad. Sci. U.S.A.* **98,** 8211–8218 (2001).

34. Courcelle, J., Donaldson, J. R., Chow, K.-H. & Courcelle, C. T. DNA damage-induced replication fork regression and processing in Escherichia coli. *Science* **299,** 1064–1067 (2003).

35. Seigneur, M., Ehrlich, S. D. & Michel, B. RuvABC-dependent double-strand breaks in dnaBts mutants require recA. *Mol. Microbiol.* **38,** 565–574 (2000).

36. Postow, L. *et al.* Positive torsional strain causes the formation of a four-way junction at replication forks. *J. Biol. Chem.* **276,** 2790–2796 (2001).

37. Bugreev, D. V., Rossi, M. J. & Mazin, A. V. Cooperation of RAD51 and RAD54 in regression of a model replication fork. *Nucleic Acids Res.* **39,** 2153–2164 (2011).

38. Gari, K., Décaillet, C., Delannoy, M., Wu, L. & Constantinou, A. Remodeling of DNA replication structures by the branch point translocase FANCM. *Proc. Natl. Acad. Sci. U.S.A.* **105,** 16107–16112 (2008).

39. Kile, A. C. *et al.* HLTF's Ancient HIRAN Domain Binds 3' DNA Ends to Drive Replication Fork Reversal. *Mol. Cell* **58,** 1090–1100 (2015).

40. Ciccia, A. *et al.* Polyubiquitinated PCNA recruits the ZRANB3 translocase to maintain genomic integrity after replication stress. *Mol. Cell* **47,** 396–409 (2012).

41. Yuan, J., Ghosal, G. & Chen, J. The HARP-like domain-containing protein AH2/ZRANB3 binds to PCNA and participates in cellular response to replication stress. *Mol. Cell* **47,** 410–421 (2012).

42. Fugger, K. *et al.* FBH1 Catalyzes Regression of Stalled Replication Forks. *Cell Rep* **10,** 1749–1757 (2015).

43. Bétous, R. *et al.* SMARCAL1 catalyzes fork regression and Holliday junction migration to maintain genome stability during DNA replication. *Genes Dev.* **26,** 151–162 (2012).

44. Ait Saada, A. *et al.* Unprotected Replication Forks Are Converted into Mitotic Sister Chromatid Bridges. *Mol. Cell* **66,** 398–410.e4 (2017).

45. Berti, M. *et al.* Human RECQ1 promotes restart of replication forks reversed by DNA topoisomerase I inhibition. *Nat. Struct. Mol. Biol.* **20,** 347–354 (2013).

46. Bhowmick, R., Minocherhomji, S. & Hickson, I. D. RAD52 Facilitates Mitotic DNA Synthesis Following Replication Stress. *Mol. Cell* **64,** 1117–1126 (2016).

47. Sotiriou, S. K. *et al.* Mammalian RAD52 Functions in Break-Induced Replication Repair of Collapsed DNA Replication Forks. *Mol. Cell* **64,** 1127–1134 (2016).

48. Wang, A. T. *et al.* A Dominant Mutation in Human RAD51 Reveals Its Function in DNA Interstrand Crosslink Repair Independent of Homologous Recombination. *Mol. Cell* **59,** 478–490 (2015).

49. Chan, Y.-L. & Bishop, D. K. Purification of Saccharomyces cerevisiae Homologous Recombination Proteins Dmc1 and Rdh54/Tid1 and a Fluorescent D-Loop Assay. *Meth. Enzymol.* **600,** 307–320 (2018).

50. Jayathilaka, K. *et al.* A chemical compound that stimulates the human homologous recombination protein RAD51. *Proc. Natl. Acad. Sci. U.S.A.* **105,** 15848–15853 (2008).

51. Yata, K. *et al.* Plk1 and CK2 act in concert to regulate Rad51 during DNA double strand break repair. *Mol. Cell* **45,** 371–383 (2012).

52. Mason, J. M. *et al.* The RAD51-stimulatory compound RS-1 can exploit the RAD51 overexpression that exists in cancer cells and tumors. *Cancer Res.* **74,** 3546–3555 (2014).

53. Bennardo, N., Cheng, A., Huang, N. & Stark, J. M. Alternative-NHEJ is a mechanistically distinct pathway of mammalian chromosome break repair. *PLoS Genet.* **4,** e1000110 (2008).

FIGURE LEGENDS

Figure 1. hsRAD51-II3A retains ssDNA binding activity, but is defective for HR. (a) Human RAD51 binding to ssDNA was determined by fluorescence polarization. Protein at various concentrations was incubated with fluorescein-tagged 84-mer ssDNA (200 nM nucleotides or 2.4 nM molecules) in buffer B and incubated at 37˚C for 30 min. Error bars represent standard deviation from triplicate experiments. The apparent Kd for hsRAD51-WT is 57 ± 1 nM, for hsRAD51-II3A is 132 ± 5 nM. (b) The D-loop activity of hsRAD51-WT and hsRAD51-II3A was measured in the presence of increasing concentrations of protein. Upper panel: autoradiogram following electrophoretic separation of D-loops from free ^{32}P-labelled ssDNA oligo substrate. Lower panel: quantitation of the autoradiogram shown in the upper panel. Error bars represent standard deviation from triplicate experiments. (c) Images depict immuno-staining RAD51 in cells prepared for staining 8 hours after a dose of 6 GY x-rays in the indicated samples. Green-RAD51 Blue-DNA. Scale bar= 5 μm (d) Quantitation of RAD51 foci after the indicated samples. Red line represents the mean. (e) DR-GFP assay. The percentage of GFP positive cells in each sample are graphed. Error bars represent SEP.

Figure 2. hsRAD51-II3A promotes DNA2-dependent processing of replication forks. (a) Box plot represents the length of CldU tracts measured after the indicated treatment. Lines represent the means for each set of measurements. Schematic of experimental design is shown above the graph. (b) Box plot represents the IdU/CldU ratio of tracts measured after the indicated treatment. Lines represent the median for each set of measurements. Schematic of experimental design is shown above the graph

Figure 3. Replication restart defects in hsRAD51-II3A expressing cells after treatment with HU. Graphs depict the percentage of replication forks that restart after the indicated treatments (left) or the percentage of new origin firings (right). Error bars represent SE. Schematic of experimental design is above the graphs.

Figure 4. hsRAD51-II3A expressing cells accumulate 53BP1 foci after treatment with HU. Representative images depicting 53BP1 foci (green) in PCNA (red) positive cells after the indicated treatments. DNA is stained in blue. Scale bar= 5 μm. Dot plot depicts quantitation of 53BP1 foci after indicated treatments. Red line represents the mean.

Figure 5. Model depicting role of RAD51 at stalled replication forks. RAD51 binds to a stalled replication fork and stabilizes by preventing extensive ssDNA formation. Proteins such as SMARCL1 and FBH1 promote replication fork reversal resulting in the formation of the chicken foot structure. Once the block is removed, helicases such as RECQ1 resolve the chicken foot structure reinstating the fork. DNA2 resects the middle toe providing a substrate for RAD51 strand-exchange dependent fork restart. DNA2 also promotes degradation of nascent strands after fork reversal in cells expressing hsRAD51-WT or hsRAD51-II3A (not depicted). In RAD51 depleted cells (RAD51 KD), the replication fork contains excess ssDNA due to uncoupling (Blue Box). hsRAD51-II3A is able to prevent MRE11-degradation by binding directly to the middle toe. hsRAD51-II3A is unable to restart the fork via strand exchange activity resulting in trapped replication intermediate resulting formation of a one-ended DSB by endonucleolytic cleavage (pink box).

Supplemental Figure 1. Cells over-expressing hsRAD51-WT or hsRAD51-II3A. (a) Purified hRad51-WT (25 μg) and hRad51-II3A mutant (10 μg) were analyzed on a 12% SDS-PAGE and the proteins were stained with Coomassie brilliant blue R250. (b) Western blot depicting levels of RAD51 after indicated treatments. TUBULIN was used as a loading control. The level of RAD51 protein levels (normalized to TUBULIN) relative to the siNS control are indicated below the blot. (c) Representative images of RAD51 fibers (non-damage associated complexes) in a small subpopulation of cells transfected with hsRAD51-WT or hsRAD51-II3A expression constructs Green- RAD51. Blue-DNA. Scale bar = 5 μm. (d) Depiction of the DR-GFP assay to measure homologous recombination in cells.

The GFP coding sequence is disrupted by an I-SceI nuclease site and contains an internal GFP fragment downstream. Repair of the I-SceI induced DSB by HR restores the GFP coding sequence. Thus, HR efficiency is measured by determining the percentage of cells expressing GFP

Supplemental Figure 2. **MRE11 dependent degradation in RAD51C-fibroblasts.** (a) Western depicting level of DNA2 after the indicated treatments. TUBULIN was used as a loading control. (b) CldU tract length in RAD51C-deficient fibroblasts after the indicated treatment. Untreated cells were used as controls. Schematic of experimental design is depicted above the graphs.

Supplemental Figure 3. 53BP1 accumulates in cells after 24 hours of HU treatment. Representative images depicting 53BP1 foci (green) in PCNA (red) positive cells after treatment with 4mM HU for 24 hours. DNA is stained in blue. Scale bar= 5 μm. Dot plot depicts quantitation of 53BP1 foci in the indicated cell lines. Red line represents the mean.

Figure 1

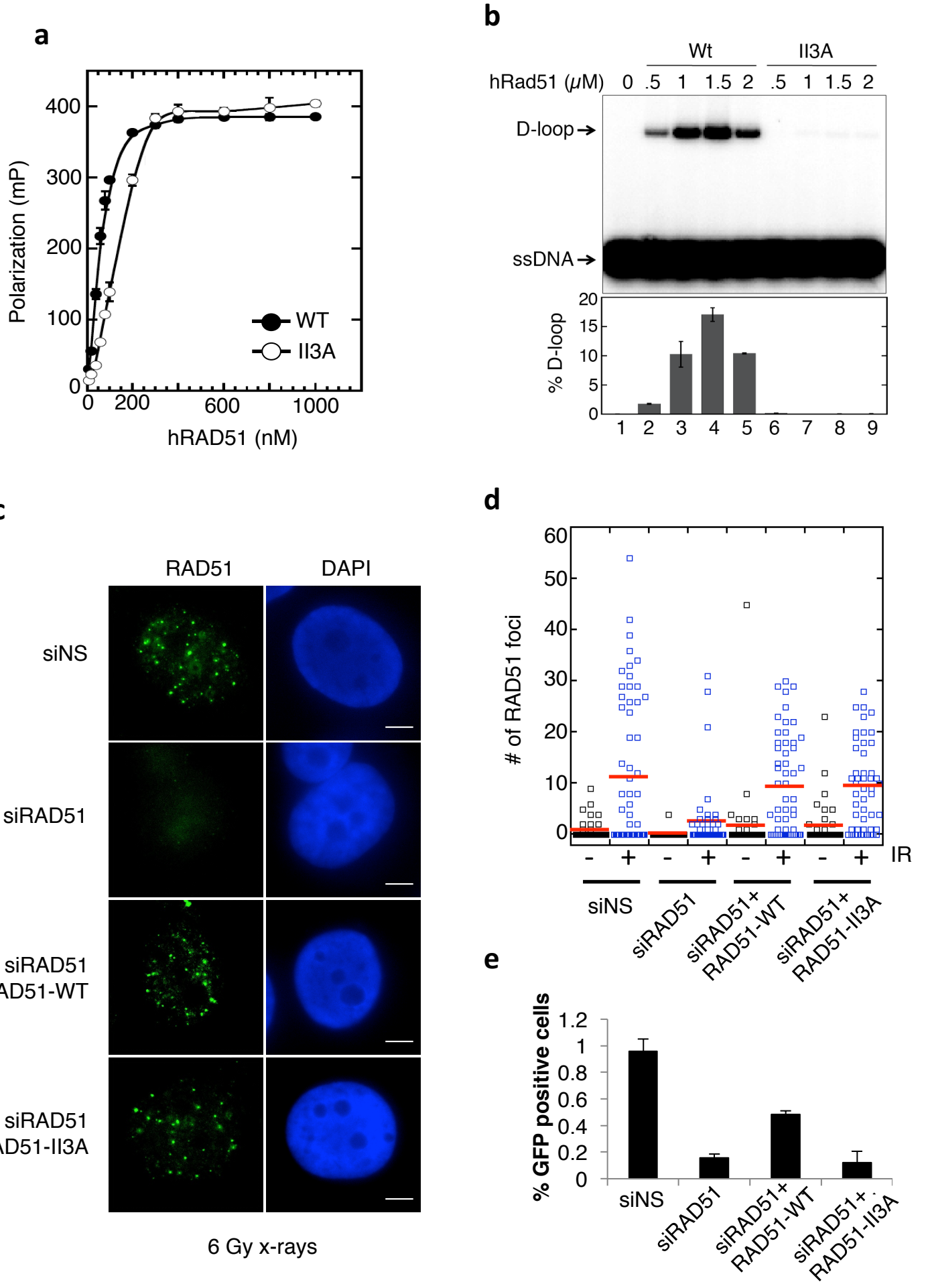

Figure 2

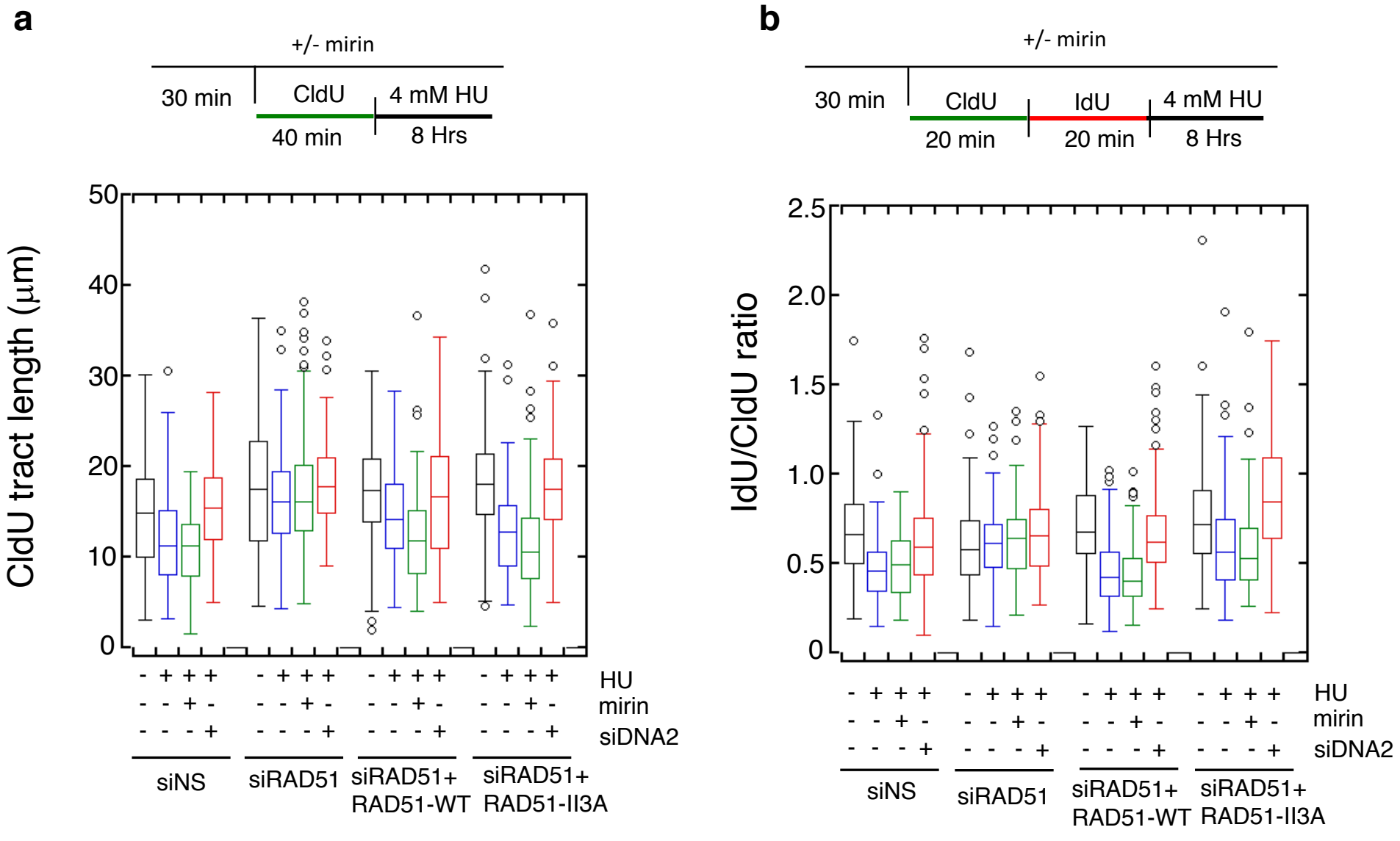
a
+/- mirin
30 min
CldU
4 mM HU
40 min
8 Hrs
CldU tract length (μm)
50
40
30
20
10
0
HU
mirin
siDNA2
siNS
siRAD51
siRAD51+ RAD51-WT
siRAD51+ RAD51-II3A
b
+/- mirin
30 min
CldU
IdU
4 mM HU
20 min
20 min
8 Hrs
IdU/CldU ratio
2.5
2.0
1.5
1.0
0.5
0
HU
mirin
siDNA2
siNS
siRAD51
siRAD51+ RAD51-WT
siRAD51+ RAD51-II3A

Figure 3

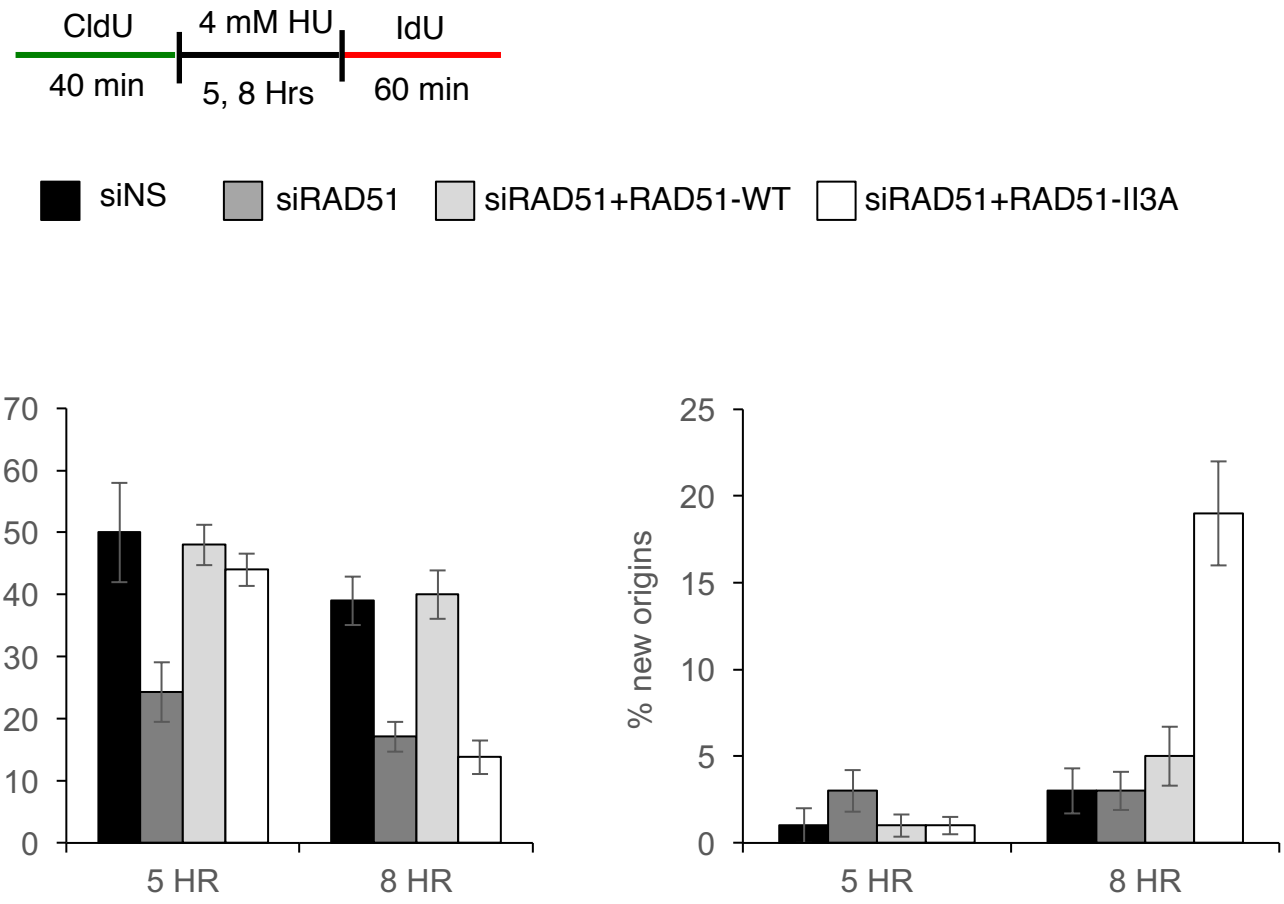

Figure 4

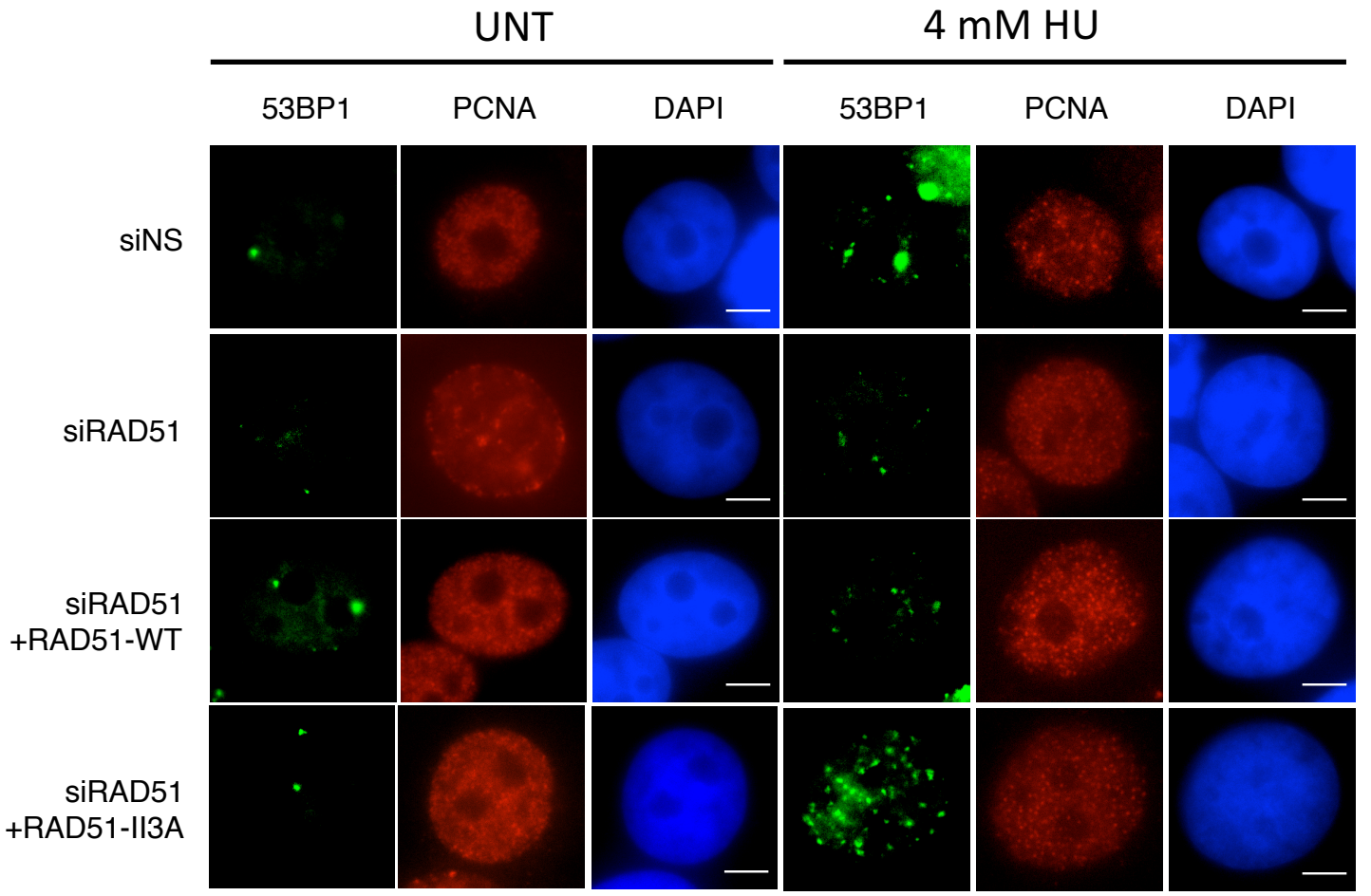

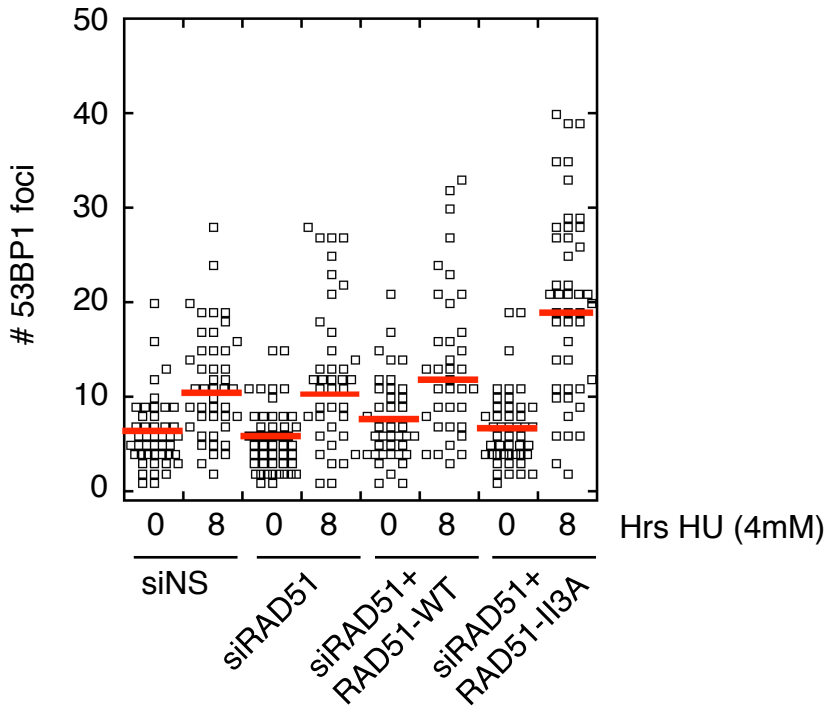

Figure 5

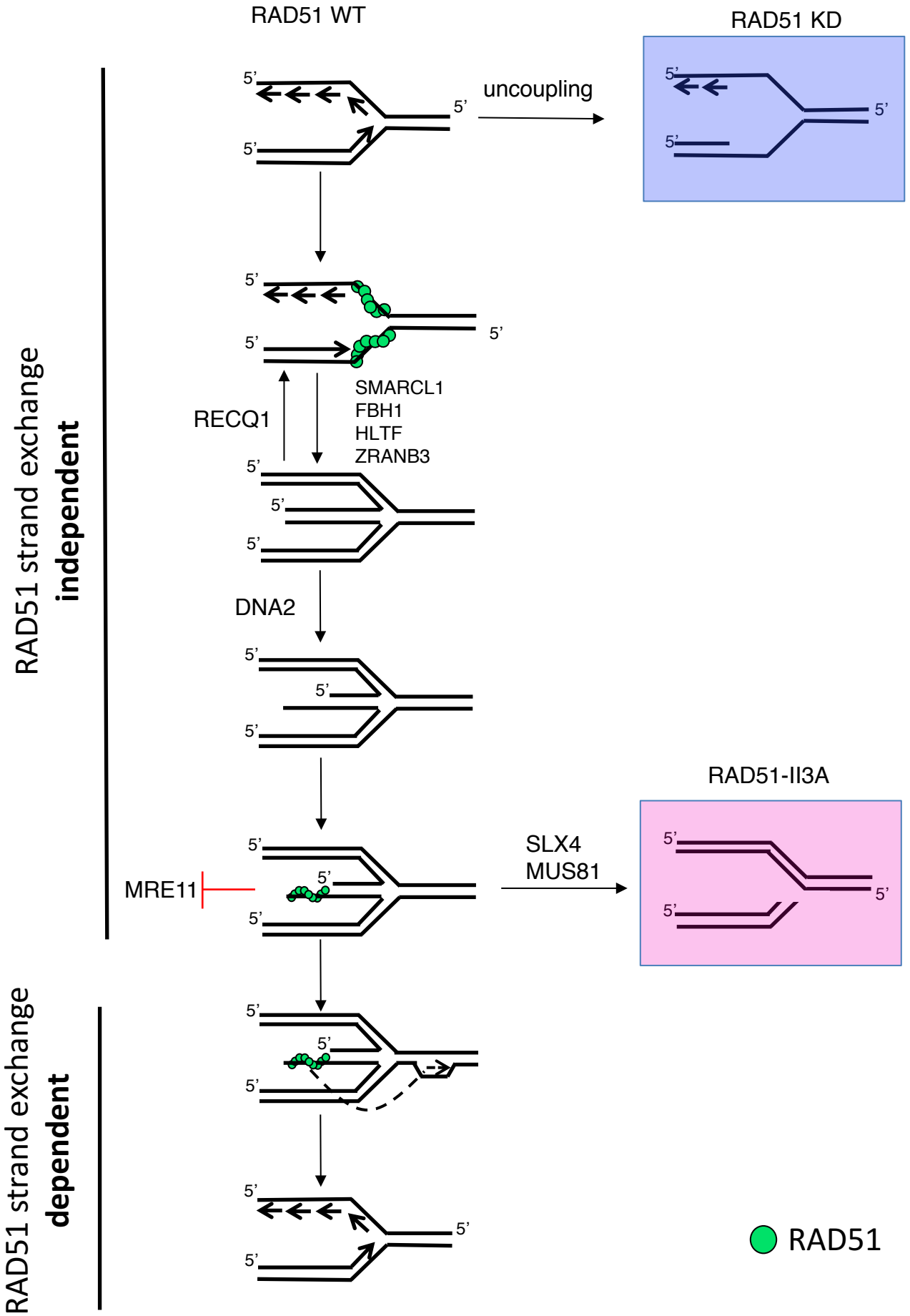
RAD51 WT
RAD51 KD
uncoupling
5'
RECQ1
SMARCL1
FBH1
HLTF
ZRANB3
DNA2
MRE11
SLX4
MUS81
RAD51-II3A
RAD51 strand exchange
independent
RAD51 strand exchange
dependent
RAD51

Supplemental Figure 1

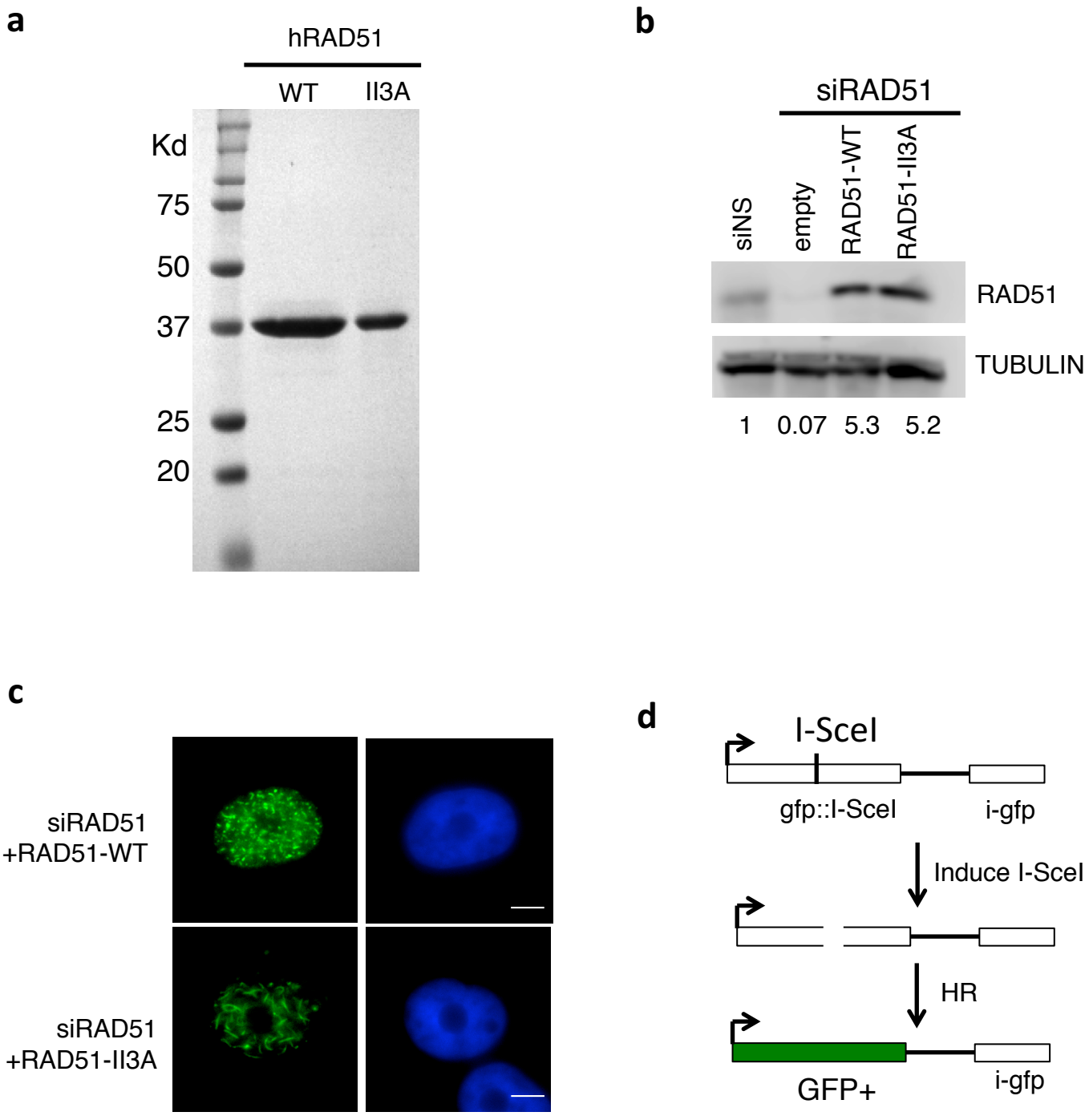

Supplemental Figure 2

a

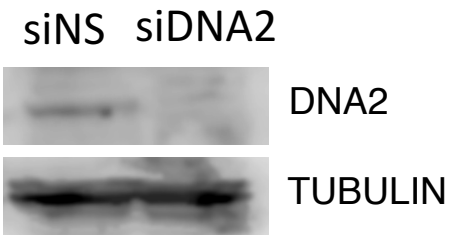

b

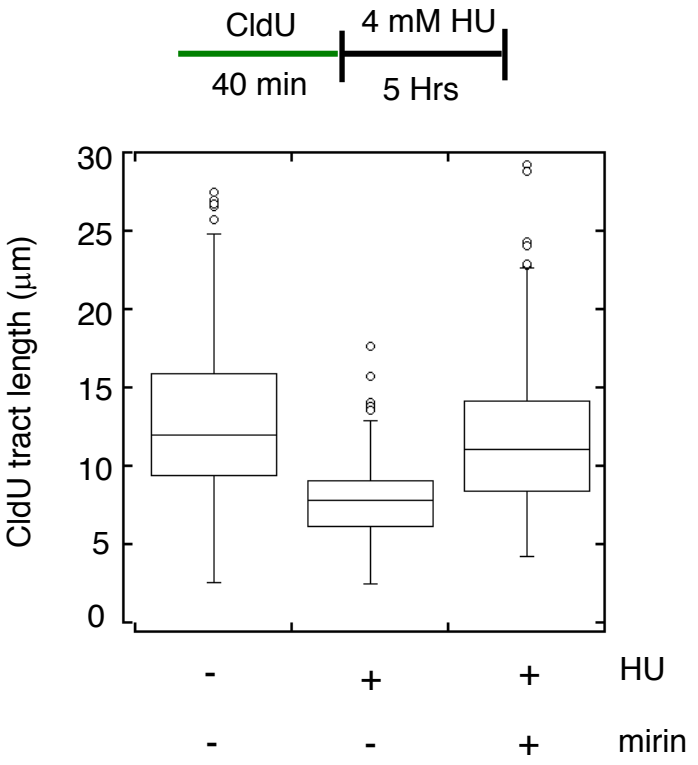

Supplemental Figure 3